Adaptive Imbalances Correction in LINC Transmitters

Paloma García, Jesús de Mingo, Antonio Valdovinos and Alfonso Ortega

University of Zaragoza, Electronics Engineering and Communications Dep., Zaragoza, Spain.
e-mail: paloma@unizar.es, mingo@unizar.es, toni@unizar.es, ortega@unizar.es

***Abstract*: The *LI*near amplification using *N*onlinear *C*omponents (LINC) technique is a well-known power amplifier linearization method to reduce adjacent channel interference in a nonconstant envelope modulation system. Its major drawback is the inherited sensitivity to gain and phase imbalances between the two amplifier branches. In this paper two novel adaptive full-digital base band methods are described which correct any gain and phase imbalances in LINC transmitters. Their main advantage is the ability to track the input signal variations and adapt to the changes of amplifier nonlinear characteristics.**

1. Introduction

The growing demand for mobile communications services and the limit of the frequency spectrum have increased the use of spectrally efficient modulations, most of which have non-constant envelopes. As a result of transmitter nonlinearities (mainly from the power amplifier) the transmitted signal spectrum expands into adjacent channels, an effect known as ACI (Adjacent Channel Interference). Some systems are very restrictive with regard to spurious emission in the adjacent channel. In order to meet this restrictive requirement, the LINC classical linearizing technique for power amplifiers is proposed (see Fig. 1). Its major drawback is inherited sensitivity to gain and phase imbalances between the two amplifier branches [1,2]. The presented novel methods use adaptive signal processing techniques and its main advantage is to track input signal variations and possible changes due to temperature variations and component aging, among others. It is carried out in base-band and is full-digital. Thorough simulations were carried to evaluate several options.

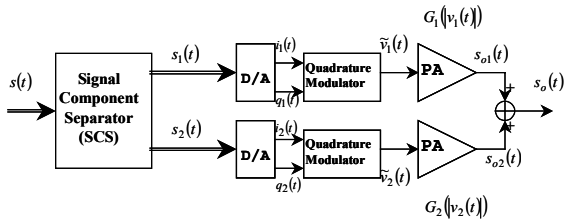

Fig.1 Schematic diagram of the LINC transmitter

2. Imbalance effects in a LINC transmitter

One of the reasons that the LINC transmitter has not been used widely is the difficulty to achieve accurate gain and phase matching required between the two paths. Errors in gain and/or phase matching will cause incomplete cancellation of unwanted elements in wideband phase modulated signals. As a result, a large number of unwanted spurious products appear in the output spectrum, as observed previously [1,2,3,4,8].
The effect of gain and phase imbalances between the two paths may be analyzed as follows. The source signal may be written in complex general format as [7]

$$s(t) = c(t)e^{j\rho(t)} \qquad 0 < c(t) \le c_{\max} \tag{1}$$

The source signal is separated into two constant-envelope signals by a Signal Component Separator (SCS) as shown in Fig.1. These signals are calculated as

$$\begin{aligned} s_1(t) &= \frac{s(t)}{2}\left[1 - e_s(t)\right] \\ s_2(t) &= \frac{s(t)}{2}\left[1 + e_s(t)\right] \end{aligned} \tag{2}$$

where $e_s(t)$ is a signal that is in quadrature to the source signal $s(t)$.

$$e_s(t) = j\sqrt{\left[\frac{c_{\max}^2}{|s(t)|^2} - 1\right]} \tag{3}$$

Thus $s(t) = s_1(t) + s_2(t)$ and $|s_1(t)| = |s_2(t)|$

The amplifier of each path is characterized by a level-dependent complex gain, with an output signal in each path given by

$$\begin{aligned} s_{o1}(t) &= v_1(t) \cdot G_1\left(|v_1(t)|\right) \\ s_{o2}(t) &= v_2(t) \cdot G_2\left(|v_2(t)|\right) \end{aligned} \tag{4}$$

where $v_1(t)$ and $v_2(t)$ are the complex baseband representation of the instantaneous input complex modulation envelope of the power amplifier in each path. In Fig.1, the power amplifier input signals, $\tilde{v}_1(t)$ and $\tilde{v}_2(t)$, represent the corresponding bandpass signals of each path. Therefore, if the D-to-A converters and quadrature modulators are supposed to be ideals, that is, $s_1(t) = \tilde{v}_1(t)$ and $s_2(t) = \tilde{v}_2(t)$, the output signal in complex format then becomes

$$\begin{aligned} s_o(t) &= s_{o1}(t) + s_{o2}(t) = s_1(t) \cdot G_1\left(|v_1(t)|\right) + s_2(t) \cdot G_2\left(|v_2(t)|\right) = \\ &= s(t)\frac{G_1\left(|v_1(t)|\right) + G_2\left(|v_2(t)|\right)}{2} + e_s(t)\frac{G_1\left(|v_1(t)|\right) - G_2\left(|v_2(t)|\right)}{2} \end{aligned} \tag{5}$$

The second term in (5) implies that there is an unwanted residual signal due to imperfect cancellation (it tends to zero as the gain and phase matching are perfected). The term introduces interfering power in the adjacent channel limiting the spectrum efficiency of the system. The aim of this method is to reduce the factor $[G_1(|v_1(t)|) - G_2(|v_2(t)|)]$ as much as possible.

3. Model of Correction Method-I

A schematic diagram of the simulation model is depicted in Fig.2. The source signal is separated into the two constant-envelope signals by an SCS. These signals are multiplied by different complex coefficients, one for each branch (K_1 and K_2). The coefficients are computed to reduce the Adjacent Channel Interference by means of an adaptive algorithm. This algorithm needs a reference of the output signal to update the complex coefficients. Two reference signals, one for each path, $r_1(t)$ and $r_2(t)$ are obtained by means of a downconversion process of the output signals $s_{o1}(t)$ and $s_{o2}(t)$ respectively, where $1/G_{L1}$ and $1/G_{L2}$ are the downconversion gains in each path. They are calculated to adjust the range of values of the quadrature demodulator input.

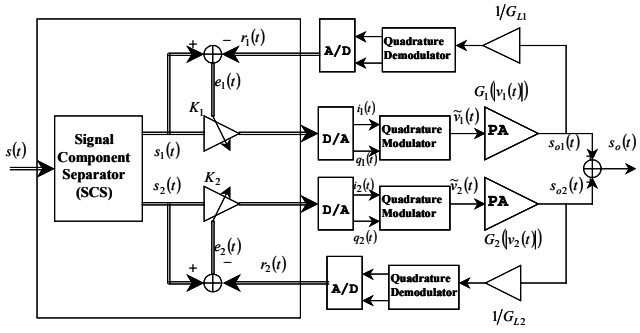

Fig.2. Simulation model

The adaptation criterion of the algorithm is to minimize the mean-squared-error in each path. The error signal for each path (defined by (6)) is the difference between the constant-envelope signal generated by the SCS block and the reference signal of the output PA signal.

$$e_1(t) = s_1(t) - r_1(t) = s_1(t)\left(1 - K_1 \frac{G_1(|v_1(t)|)}{G_{L1}}\right)$$
$$e_2(t) = s_2(t) - r_2(t) = s_2(t)\left(1 - K_2 \frac{G_2(|v_2(t)|)}{G_{L2}}\right) \qquad (6)$$

where ideal D-to-A, A-to-D converters, quadrature modulators and demodulators are assumed.

The cost functions to minimize are defined as

$$J_1 = E\left[\ |e_1(t)|^2\ \right] \qquad J_2 = E\left[\ |e_2(t)|^2\ \right] \qquad (7)$$

Where E[.] denotes the statistical expectation operator. The gradient of the cost function is calculated as

$$\nabla_{K_n} J_n = \frac{\partial J_n}{\partial Kr_n} + j\frac{\partial J_n}{\partial Ki_n} \qquad (8)$$

With $K_n = Kr_n + jKi_n \qquad n=1,2$

Where Kr_n denotes the real part and Ki_n the imaginary part of K_n.

For the cost function J_n to attain its minimum value, all the terms of the gradient must be simultaneously equal to zero. Applying some approximations, we finally get for each path the result

$$\nabla_{k_n} J_n \approx -2 \cdot E\left(e_n(t) \cdot \left(\frac{r_n(t)}{K_n}\right)^*\right) \qquad n=1,2 \qquad (9)$$

Therefore, using the instantaneous estimate of the gradient, the updated value of the adaptive coefficient at time m+1 is computed by using the simple recursive relation

$$K_n(m+1) = K_n(m) + \mu_n \cdot e_n(m) \cdot \left(\frac{r_n(m)}{K_n(m)}\right)^* \qquad n=1,2 \qquad (10)$$

Where the positive real-valued constant μ_n (step-size), controls the speed of convergence and the misadjustment (final excess error) of the algorithm.

The source signal for simulations was a $\pi/4$-DQPSK modulated signal filtered with a squared-root raised cosine with a 0.35 roll-off factor at 36 Kbps, which corresponds to a TETRA signal. The amplifier is characterized by a complex gain using a memoryless model [6,8], which depends on the input signal level. The complex gain of the amplifier is extracted from measurements of AM-AM and AM-PM conversion of a Mitsubishi M68749 amplifier (with a driver) at 390 MHz (50 Ω system). A polynomic regression is used to model the amplifier complex gain of each path.

$$G_n(|v(t)|) = M_n(|v(t)|) \cdot e^{j\Phi_n(|v(t)|)} \qquad n=1,2 \qquad (11)$$

$$\begin{aligned} M_n(|v(t)|) = {} & 200\alpha_{n,1} + 800\alpha_{n,2}|v(t)| - 12760\alpha_{n,3}|v(t)|^2 \\ & + 67930\alpha_{n,4}|v(t)|^3 - 193540\alpha_{n,5}|v(t)|^4 \\ & + 281970\alpha_{n,6}|v(t)|^5 - 162240\alpha_{n,7}|v(t)|^6 \end{aligned} \qquad (12)$$

$$\begin{aligned} \Phi_n(|v(t)|) = {} & 1.14\beta_{n,1} + 2.25\beta_{n,2}|v(t)| - 27.67\beta_{n,3}|v(t)|^2 \\ & + 147.24\beta_{n,4}|v(t)|^3 - 461.0754\beta_{n,5}|v(t)|^4 \\ & + 722.6528\beta_{n,6}|v(t)|^5 - 432.1345\beta_{n,7}|v(t)|^6 \end{aligned} \qquad (13)$$

The amplifier in path 1 is simulated with the coefficients α=1 and β=1. The amplifier in path 2 was simulated introducing several imbalances in some coefficients of the gain and phase polinomy. Several tests were carried out by modifying the factors $\alpha_{2,j}$ and $\beta_{2,j}$ among a ± 10%. Fig. 3 shows the normalized input *S(f)* and output $S_o(f)$ power spectrum density for a 3-Watt output power amplifier under different gain and phase imbalances between both branches of the LINC transmitter (without applying the correction method).

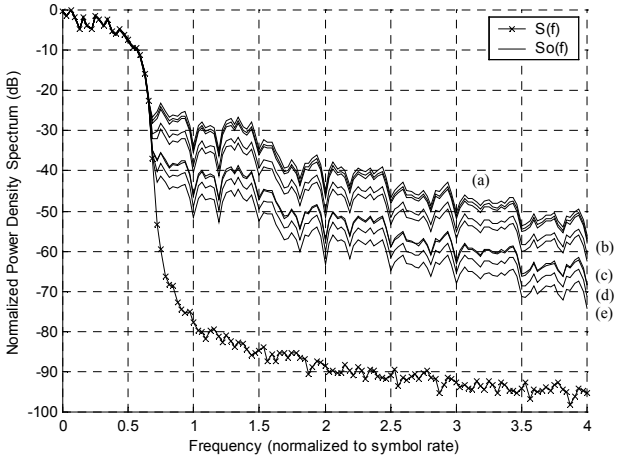

Fig. 3. Normalized Power Density Spectrum of simulated input S(f) and output S_o(f) with several gain and phase imbalances between both branches of a LINC transmitter without correction method. (a) ΔG_a≈3dB, $\Delta\phi_a$≈10º, (b) ΔG_a≈2dB, $\Delta\phi_a$≈5º,(c) ΔG_a≈1dB, $\Delta\phi_a$≈3º, (d) ΔG_a≈0.7dB, $\Delta\phi_a$≈2º,(e) ΔG_a≈0.5dB, $\Delta\phi_a$≈2º

Fig. 3 illustrates the effect of gain and phase imbalances and the need for a method to achieve gain and phase matching as presented in this paper.

Fig. 4 compares the normalized input and output power spectrum density with and without the presented adaptive correction method and with a gain imbalance of approximately 1.5 dB and a phase imbalance around 5º between the amplifier in path 1 and the one in path 2. The ACI is improved after applying the correction method with accurate gain and phase matching between the two paths. The ACI in the first adjacent channel without correction is around –35 dBc, but -70 dBc with the correction method (35 dB improvement).

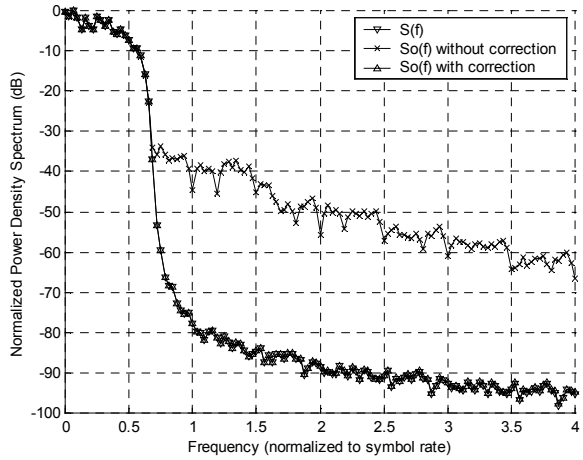

Fig. 4. Normalized Power Density Spectrum of simulated input S(f) and output S_o(f) with and without correction

3.1 Limitation of the correction algorithm

In the previous simulation the same downconversion gain in each path was assumed, that is, $G_{L1}=G_{L2}$. The practical implementation of this balance between both downconversion branches is technologically very difficult, although it is easier than between LINC transmitter branches. Thus, we analyzed the effect of the imbalance (supposedly linear), between the downconversion branches. Fig. 5 shows the performance obtained in the simulation when a gain (ΔG) and phase ($\Delta\phi$) imbalance factor between G_{L1} and G_{L2} is introduced. As expected, ACI under real conditions increases considerably, with gain and phase imbalances between downconversion branches.

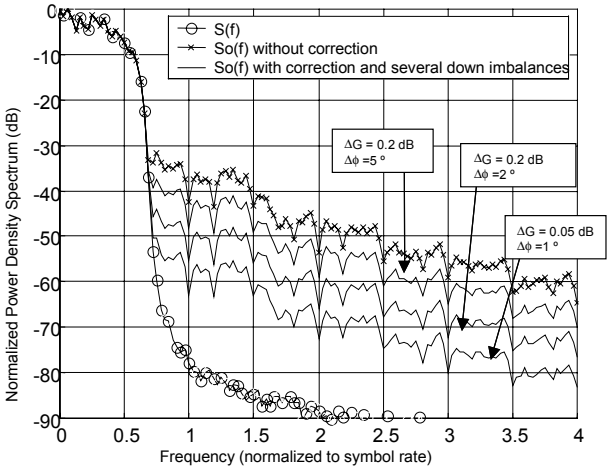

Fig. 5. Normalized Power Density Spectrum of simulated input S(f) and output S_o(f) with and without correction method and with several imbalances between downconversion branches.

4. Model of Correction Method-II

One way to solve this problem is to have only one feedback branch, thus obtaining a single reference signal of the power output signal, $s_o(t)$. This reference signal can be split into two signals using a SCS block to obtain the two error signals (one for each path), needed for the adaptive algorithm. Fig. 6 shows the new proposed architecture.

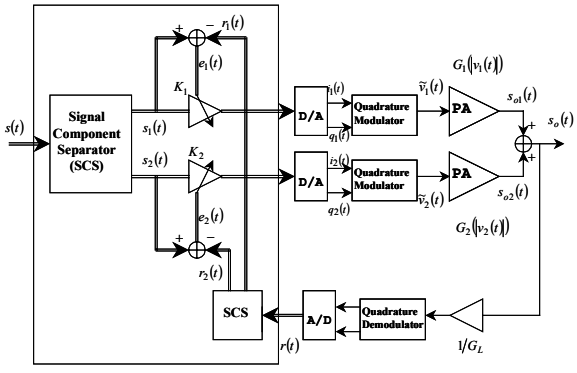

Fig.6. Simulation model of method II

In this case, the error signal in each path is

$$e_1(t) = s_1(t) - r_1(t)$$
$$e_2(t) = s_2(t) - r_2(t) \quad (14)$$

where $r_1(t)$ and $r_2(t)$ are obtained from $r(t)$ using a Signal Component Separator block
Assuming ideal D-to-A and A-to-D converters and quadrature modulators and demodulator, the reference signal $r(t)$ is

$$r(t) = r_1(t) + r_2(t) = \frac{s_o(t)}{G_L} = \frac{s_1(t)K_1G_1(|v_1(t)|) + s_2(t)K_2G_2(|v_2(t)|)}{G_L} \quad (15)$$

As in the previous method, the adaptation criterion of the algorithm is used to minimize the mean-squared-error in each path. Therefore the cost function to minimize is defined as (7). Applying some approximations, for each path we obtain the same result as (9). Therefore, the updated value of the adaptive coefficient at time m+1 can be computed using the same recursive relation as (10).

The performance of this new method is illustrated in Fig.7. The ACI in the first adjacent channel without correction is around –35 dBc, but below –64 dBc using the new correction method (≈30dB improvement). It gets worse than the previous method, but it does not depend on the downconversion gain imbalances and only one feedback demodulation branch is needed.

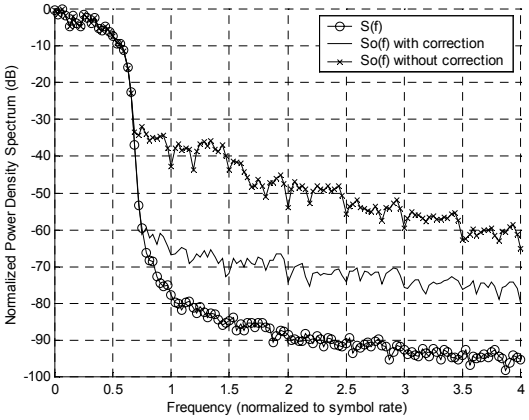

Fig. 7. Normalized Power Density Spectrum of simulated input S(f) and output $S_o(f)$ with and without correction method II

The speed of convergence can be measured by analyzing the time evolution of the error signals $e_1(t)$ and $e_2(t)$. The step size parameter, μ_n, was chosen to reduce the ACI (up to -60dBc in the first adjacent channel) as quickly as possible (see Fig. 8). The convergence time (< 1μs) is suitable in order to be implemented in a real time system.

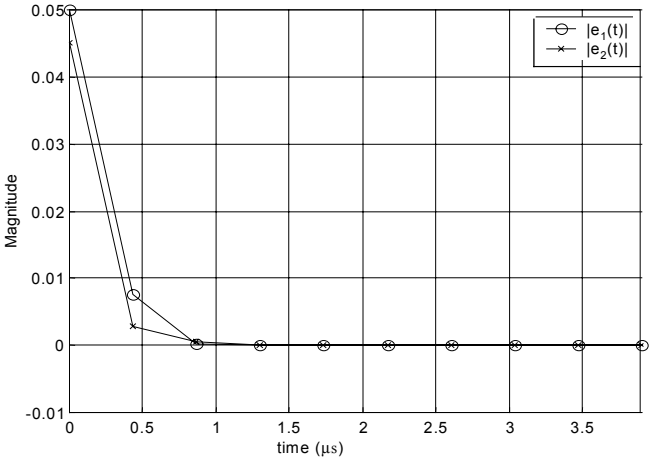

Fig. 8. Evolution of the error signals in each path.

4.1. Modulator and Demodulator Misalignments

Perfectly balanced quadrature modulators and demodulator were assumed in this architecture, which leads to another practical consideration. The quadrature imbalances (amplitude and phase) create a residue in the adjacent channel, increasing the ACI [9]. Fig. 9 shows the degradation of the ACI when there are imbalances in the quadrature modulators. Simulations were carried out with several amplitude and phase imbalances. The results are very promising for imbalance values corresponding to commercial quadrature modulators (amplitude error between 0.5 dB and 1 dB and phase error between 2º and 5º). We also analyzed the effect of an unbalanced quadrature demodulator in this architecture. Some simulations were carried out with commercial gain and phase errors but their effect on the I/Q demodulator was not significant.

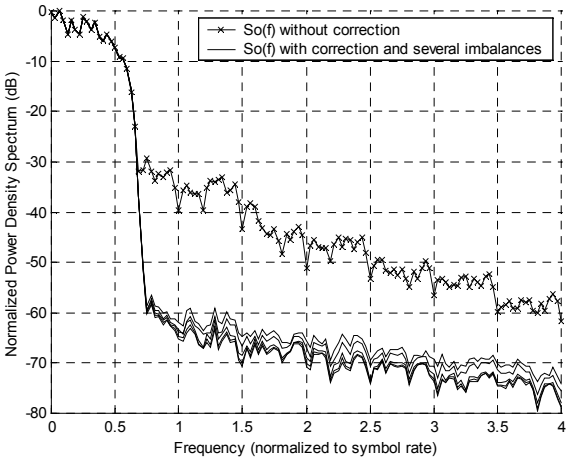

Fig. 9. Normalized Power Density Spectrum of simulated input S(f) and output $S_o(f)$ with several gain and phase imbalances in the quadrature modulator.

4.2. Method Viability

According to the simulations presented, the method performs well even with imbalances in the quadrature modulator and demodulator. In this section we discuss the practical feasibility of the method.

Digital blocks of the design (such as SCS) and the calculation to update the adaptive coefficients K_1 and K_2 can be implemented in a powerful Digital Signal Processor (DSP) device. Maximum optimization of the implementation of these algorithms is carried out approaching some DSP features, such as speed or special instructions for signal processing. The algorithms must be researched in order to decrease the number of instructions to reduce the computational load and introduce minimum delay in the system.

Another important effect can be the quantization in the SCS block. The design is carried out according to the requirements described in [5], and therefore the effect of the quantization will be minimum. The Signal Component Separator is implemented in a fixed-point DSP of a finite word length (16 bits). According to [5] this word length is suitable enough to obtain an ACI up to –60 dBc in the first adjacent channel. The effect quantization will not be a problem in a real design with a right choice of D-to-A and A-to-D converters in the current wide range of commercial devices (e.g. 14 or 16 bits).

Another ideal situation that has been assumed in the previous simulations corresponds to the nonzero loop delay. The reference signal $r(t)$ is a delayed and attenuated version of amplifier output $s_o(t)$. The delay must be compensated for the adaptive algorithm to correctly compare $s_n(t)$ with $r_n(t)$. The same DSP device generates signals $s_n(t)$ and $r_n(t)$, where $s_n(t)$ are obtained from the source signal $s(t)$ and $r_n(t)$ from the feedback signal $r(t)$. Thus, the delay compensation can be easily obtained by comparing the samples with the calculated loop delay. Therefore the delay produced by the correction circuit has to be estimated before introducing the adaptive algorithm. A rough estimation can be carried out with the theoretical time delay of the components in the design or by applying some of the loop delay estimation techniques proposed by other authors [6,8,10,11] or with some previous calibration.

5. Conclusion

A novel method to correct gain and phase imbalances in LINC transmitters was described. Using a simulation we showed that it is possible to reduce the ACI to meet the restrictive specifications of the TETRA digital communication system. The system converges quickly towards very low interference levels in adjacent channels. As a result of its adaptive technique, this method can track the input signal variations and possible changes due to variations in operating conditions. According to the simulation, the adaptive coefficient quickly reaches its optimal value, therefore this method could be implemented in a real system by means a suitably powerful DSP device.

Acknowledgements

This work has been supported by the CICYT (Spain) under grant TIC2001-2481.

REFERENCES

[1] F. J. Casadevall and A. Valdovinos, "Performance Analysis of QAM Modulations Applied to the LINC Transmitter", *IEEE Trans. on Veh. Tech., Vol. 42, No. 4, November 1993, pp. 399-406*

[2] F. J. Casadevall and J.J. Olmos, "On the behaviour of the LINC Transmitter", in Proc. 40th *IEEE Veh. Tech. Conf, Orlando. May 6-9 1990. pp 29-34*

[3] L. Sudström. "Automatic adjustment of gain and phase imbalances in LINC transmitters", *Electron. Lett., Vol. 31, no 3, pp. 155-156, Feb 2, 1995*.

[4] Xuejun Zhang and Lawrence E. Larson, "Gain and phase error-free LINC transmitter", *IEEE Trans. on Veh. Tech., Vol. 49, No. 5, September 2000, pp. 1986-1994*.

[5] L. Sundström, "The Effect of Quantization in a Digital Signal Component Separator for LINC Transmitters", *IEEE Trans. on Veh. Tech., Vol. 45, No. 2, May 2000, pp. 346-352*.

[6] S.A. Maas, "Volterra analysis of spectral regrowth", *IEEE Microwave Guided Wave Lett, vol. 7, pp. 192-193, July 1997*

[7] Hetzel, S.A., A. Bateman, and J.P. McGeehan, " LINC transmitter", *IEEE Electronics Letters, vol. 27, no 10, pp. 844-846, May 1991*

[8] J. de Mingo and A. Valdovinos, "Performance of a New Digital Baseband Predistorter Using Calibration Memory", *IEEE Trans. on Veh. Tech., Vol. 50, No. 4, July 2001, pp. 1169-1176*

[9] J. K. Cavers, "The effect of quadrature modulator and demodulator errors on adaptive digital predistorters for amplifier linearization", *IEEE Trans. on Veh. Tech., Vol. 46, May 1997, pp. 456-466*

[10] J. K. Cavers, "New methods for adaptation of quadrature modulators and demodulator in amplifier linearization circuits", *IEEE Trans. on Veh. Tech., Vol. 46, No 3, Aug. 1997, pp. 707-716*

[11] Y. Nagata, "Linear amplification technique for digital mobile communications" *Proc. 39th IEEE Veh. Conf., pp159-164, May 1989*